AIP | Applied Physics Letters

Extremely low surface recombination velocities in black silicon passivated by atomic layer deposition

Martin Otto, Matthias Kroll, Thomas Käsebier, Roland Salzer, Andreas Tünnermann et al.

Citation: Appl. Phys. Lett. **100**, 191603 (2012); doi: 10.1063/1.4714546
View online: http://dx.doi.org/10.1063/1.4714546
View Table of Contents: http://apl.aip.org/resource/1/APPLAB/v100/i19
Published by the American Institute of Physics.

Extremely low surface recombination velocities in black silicon passivated by atomic layer deposition

Martin Otto,[1,a)] Matthias Kroll,[2] Thomas Käsebier,[2] Roland Salzer,[3] Andreas Tünnermann,[2] and Ralf B. Wehrspohn[1,3]
[1]*Martin-Luther-University Halle-Wittenberg, μMD Group-Institute of Physics, Heinrich-Damerow-Strasse 4, 06120 Halle, Germany*
[2]*Friedrich-Schiller-Universität Jena, Institute of Applied Physics, Max-Wien-Platz 1, 07743 Jena, Germany*
[3]*Fraunhofer Institute for Mechanics of Materials Halle, Walter-Hülse-Str. 1, 06120 Halle, Germany*

(Received 1 March 2012; accepted 25 April 2012; published online 9 May 2012)

We investigate the optical and opto-electronic properties of black silicon (b-Si) nanostructures passivated with Al_2O_3. The b-Si nanostructures significantly improve the absorption of silicon due to superior anti-reflection and light trapping properties. By coating the b-Si nanostructures with a conformal layer of Al_2O_3 by atomic layer deposition, the surface recombination velocity can be effectively reduced. We show that control of plasma-induced subsurface damage is equally important to achieve low interface recombination. Surface recombination velocities of $S_{eff} < 13\,cm/s$ have been measured for an optimized structure which, like the polished reference, exhibits lifetimes in the millisecond range. © *2012 American Institute of Physics*. [http://dx.doi.org/10.1063/1.4714546]

Nanostructured silicon surfaces can strongly enhance absorption throughout the whole spectral range above the energy gap of a silicon solar cell. In particular, black silicon (b-Si) is far more effective than conventional antireflection coatings (ARCs).[1–3] However, low charge carrier lifetimes and high surface recombination velocities in such devices strongly limit the device performance up to now. The structuring of the silicon surface leads to enhanced recombination rates due to the larger surface area and a lower bulk lifetime close to the surface as a consequence of defects introduced during the fabrication process.[4,5] Thus, the efficiency of solar cells based on b-Si is inferior to that of state-of-the-art solar cells.[6–9] The only way to overcome this drawback is to reduce the introduced surface damage during the fabrication process as well as to effectively passivate the structured Si surface. In the last years, Al_2O_3 deposited by atomic layer deposition (ALD) was intensively studied because a conformal thin surface layer of Al_2O_3 very effectively improves the surface passivation.[10–14] ALD deposition and annealing of this dielectric layer lead to an excellent chemical passivation due to strong coordination of Si and O at the interface[15,16] and selective hydrogenation.[17] This leads to a very low density of defect states at the interface.[17] Moreover, an extremely high concentration of fixed negative charges has been measured providing a strong backsurface field.[12]

In this work, b-Si was fabricated by plasma etching of silicon.[18] We used wet chemical cleaning and deposited the Al_2O_3 conformally on the b-Si by thermal ALD. To activate the passivation, a postdeposition annealing treatment was carried out. For certain b-Si geometries, lifetimes in the millisecond range could be measured.

Black silicon was structured by inductively coupled plasma reactive ion etching (ICP-RIE) using SF_6 and O_2.[19] Three different b-Si structures were fabricated for this work by varying process pressure or etching time. Nanostructuring was applied bifacially to produce identical surface conditions on both the front and rear of polished Czochralski-grown (CZ) Si wafers. The 6″ diameter wafers were boron-doped (1–5 Ωcm) and had thicknesses between 350 μm and 450 μm. The nanostructures originate from overlapping etch pits and consist of sharp needle-like features with characteristic heights of approximately 500 nm, 600 nm, and 1700 nm, respectively. In the following, these will be called shallow, intermediate and deep b-Si structure. The aspect ratios of the structures are about 3, 4, and 10, respectively. Prior to passivation, all samples were wet chemically cleaned in (5:1:1) solutions of H_2O:NH_4OH:H_2O_2 and H_2O:HCl:H_2O_2 at 80 °C for 10 min. Between the two cleaning steps the samples were dipped in 5 vol. % HF at room temperature for 60 s. After the second cleaning step, the clean OH-terminated samples were transferred directly to the thermal ALD reactor where the surface passivation was performed on both sample sides simultaneously. For Al_2O_3 deposition, trimethylaluminium (TMA) and H_2O were used as precursor materials. Film thicknesses of about 100 nm were achieved during 1000 cycles at 200 °C. A postdeposition annealing step was performed at temperatures between 350 °C and 500 °C for 30 min in a low pressure Ar ambience or in normal pressure air. Independent of the surface structure or annealing atmosphere, the optimum annealing temperature for all samples was found to be between 400 °C and 425 °C in accordance to earlier reports.[20]

For the optical characterization, single-side structured samples were prepared. From those samples, both hemispherical reflectance and transmittance were measured with an integrating sphere. The reflectance spectra were normalized to a Spectralon reflectance standard. For analysis of the surface geometry and film conformity sample, cross sections were prepared by focussed ion beam (FIB) milling and examined in-situ by scanning electron microscopy (SEM). The film thickness and homogeneity were determined by ellipsometry on polished wafers at 221 measurement points. All charge carrier lifetimes were measured after annealing via the quasi-steady-state photoconduction (QSSPC) method with a Sinton WCT 120 lifetime tester.

a)Electronic mail: martin.otto@physik.uni-halle.de.

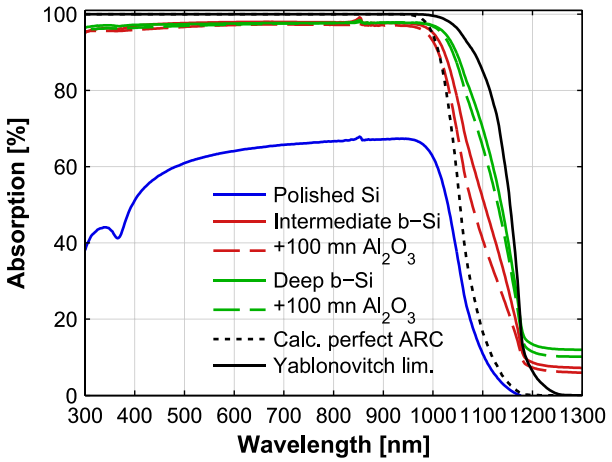

FIG. 1. Experimental absorption spectra of the intermediate (red) and deep (green) b-Si structures before (solid) and after (dashed) coating with 100 nm Al_2O_3. For comparison, the experimental absorption spectrum of a polished wafer (solid blue), as well as theoretical spectra of a perfect anti-reflection coating (dash-dotted black) and a perfect anti-reflection coating with Lambertian scattering (Yablonovitch limit, solid black) are also plotted.

The absorption spectra of the structured b-Si samples and a polished reference wafer are shown in Fig. 1. For comparison, two theoretical limits are plotted as well. The dash-dotted black line represents the absorption of a polished Si wafer without any front reflection losses assuming a hypothetical perfect ARC. The solid black line represents the Yablonivitch limit[1] where a perfect ARC and additional light trapping due to a Lambertian scattering layer are assumed. As can be seen from Fig. 1, both, the uncoated b-Si samples as well as the b-Si samples after coating with 100 nm Al_2O_3 exhibit very low reflection losses. The influence of the passivation layer on the anti-reflection properties of the structures is negligible. The absorption of the structured samples near the band edge of silicon clearly exceeds that of a polished wafer with perfect ARC, thus, proving a light trapping effect due to light scattering at the b-Si needles. The light trapping effect is only slightly diminished by the Al_2O_3 coating whereby the impact on the deep structure is the lowest. Even after coating with 100 nm, Al_2O_3 the intermediate and deep b-Si structures, respectively, reach 91% and 95% of the absorption of the Yablonovitch limit integrated over the spectral range from 300 nm to 1150 nm.

The surface geometry of the b-Si structures as well as the step coverage of the deposited films was investigated by FIB cross sections. SEM images of the intermediate and deep b-Si structures are shown in Figs. 2(a) and 2(b), respectively. Both samples have been coated perfectly conformal with 100 nm Al_2O_3 without any voids or inclusions between the passivation layer and the structured surface. The ALD films precisely reproduce the surface morphology equally well in either case of low and high aspect ratios. Despite the large film thickness, no blistering was observed after annealing on OH-terminated surfaces. Due to the irregular shape of the b-Si needles, it had been difficult to determine the exact film thickness from SEM images. Therefore, the growth rate and film homogeneity were investigated by spectroscopic ellipsometry on polished wafers. The growth per ALD cycle (gpc) was found to be 1.026 ± 0.002 Å/cycle. The RMS film thickness variation was $< 0.2\%$ on the front and $< 2\%$ on the rear of the wafer.

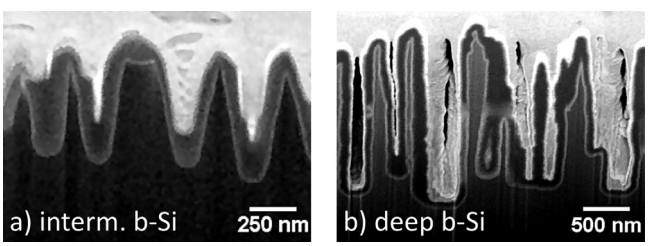

FIG. 2. SEM cross sections of the intermediate (a) and the deep (b) b-Si structure covered by thermal ALD deposited Al_2O_3 (dark grey). The bright grey line is the Si-Al_2O_3-interface. The structures were protected by Pt before cross-section preparation (white coating).

The carrier lifetimes of the shallow, intermediate, and deep b-Si structure as well as the polished reference, all coated with a 100 nm Al_2O_3 layer, were determined as a function of the excess charge carrier density by QSSPC (Fig. 3) after annealing. Considering that all samples were prepared on CZ wafers, extremely long carrier lifetimes of over $\tau_{eff} = 1.4$ ms and $\tau_{eff} = 1.6$ ms were measured on the intermediate b-Si structure and the reference wafer, respectively, at an injection level of $\Delta N = 5 \cdot 10^{15}\,cm^{-3}$. At the same level of excess charge carrier density, the shallow and deep structured samples exhibit significantly lower values of $\tau_{eff} = 500\,\mu s$ and $\tau_{eff} = 230\,\mu s$, respectively. The effective surface recombination velocity was determined by assuming an infinite bulk lifetime and is given by[11]

$$S_{eff} \leq \frac{W}{2 \cdot \tau_{eff}}$$

with τ_{eff} the effective lifetime and S_{eff} the maximum effective surface recombination velocity on either side of the wafer and W the sample thickness. Both the polished reference and the intermediate b-Si structure exhibit values of $S_{eff} \leq 12 \pm 2$ cm/s and $S_{eff} \leq 13 \pm 2$ cm/s at an injection level of $\Delta N = 5 \cdot 10^{15}\,cm^{-3}$, respectively. Lifetimes and surface recombination velocities of all b-Si structures are summarized in Table I.

In the following, the optical and electronic properties of the three b-Si structures will be discussed and a preliminary

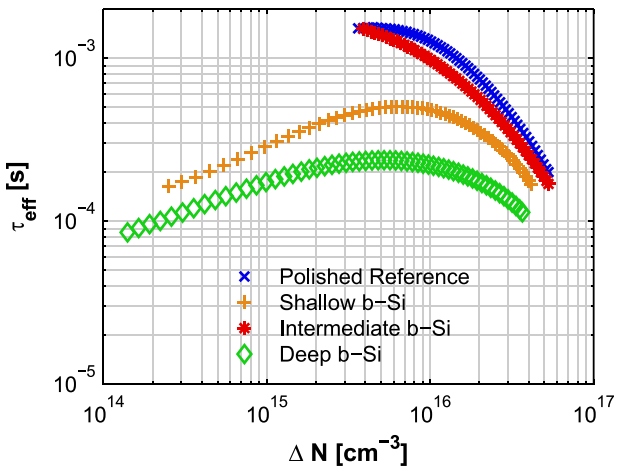

FIG. 3. Injection level dependent lifetime of the three model structures in comparison to a polished reference passivated with 100 nm of Al_2O_3. The samples were annealed in low pressure Ar ambient at 425 °C for 30 min.

TABLE I. Summary of the effective carrier lifetimes of Al_2O_3 passivated b-Si structures as shown in Fig. 3 at an excess carrier density of $\Delta N = 5 \cdot 10^{15}\,cm^{-3}$ and the corresponding S_{eff}-value assuming an infinite bulk lifetime.

Structure	Material	τ_{eff} [μs]	S_{eff} [cm/s]
Planar substrate	(CZ)	1634 ± 245	12 ± 2
Shallow b-Si	(CZ)	502 ± 76	45 ± 7
Intermediate b-Si	(CZ)	1475 ± 133	13 ± 2
Deep b-Si	(CZ)	237 ± 36	80 ± 6

model will be given why the intermediate structure has the best electronic properties. The strong near band edge absorption of the b-Si samples is attributed to pronounced scattering at the surface structures.[2] Upon transition through the structured interface a significant fraction of the incoming light is scattered into large propagation angles beyond the critical angle of total internal reflection. It then takes multiple round trips until the light is scattered back into the loss cone and might leave the wafer. This efficiently enhances the optical path length, and hence, the probability for absorption. In comparison to the theoretical limit of a perfect ARC without light trapping, the absorption at 1150 nm is enhanced by a factor of 6 and 10 for the intermediate and deep structure, respectively. The better performance of the deep b-Si sample is a result of the steeper sidewalls and an optically more favorable inter-needle spacing. Geometrically, the shallow structure exhibits very similar sidewall angles and aspect ratios like the intermediate one. The optical performance of the two structures is therefore very similar even though the electronic performance is very different. Residual absorption below the band gap energy of Si which is observed for all structured samples can be explained by free carrier absorption due to moderate boron doping of the wafers ($p \sim 3 \cdot 10^{15} - 1.4 \cdot 10^{16}\,cm^{-3}$). According to the model proposed by Green,[21] the free carrier absorption coefficient at 1200 nm for those doping concentrations is in the range of $1.1 \cdot 10^{-2}\,cm^{-1}$ to $5.5 \cdot 10^{-2}\,cm^{-1}$. This is about the same order of magnitude as the intrinsic absorption coefficient of Si at this wavelength.[22] Therefore, the experimentally observed absorption-plateau above 1200 nm in Fig. 1 is consistent with free carrier absorption enhanced by light trapping.

Comparing the light trapping efficiency of b-Si surfaces to conventional alkaline textures, our deep structure performs at least as well as inverted pyramids like introduced by Zhao *et al.*[9] With additional well suited ARCs, both, alkaline textures and b-Si show equally well anti-reflective behaviour. However, we predict better optical overall-performance of b-Si on very thin wafers ($W < 50\,\mu m$) due to stronger scattering. A more comprehensive study concerning b-Si optics can be found in the paper of Kroll *et al.*[3]

The QSSPC measurement of the intermediate b-Si structure revealed a very long carrier lifetime and a low surface recombination velocity which is comparable to that of the planar reference wafer. However, the shallow and deep b-Si structures both exhibit significantly inferior lifetimes. As determined by FIB cross sections, the quality of the Al_2O_3 passivation layer is equally good on all three structures concerning conformity. Since the geometrical parameters are very similar for the shallow and the intermediate structure, their difference in lifetime has to originate from the etching process itself. Schaefer *et al.* reported that a longer etching time in a parallel plate reactor may lead to a reduced plasma-induced damage layer.[4] Therefore, we speculate that the plasma-induced damage layer is smaller on the intermediate structure than on the shallow structure leading to a longer effective carrier lifetime. In contrast, the deep structure has been fabricated at a lower pressure than the shallow and the intermediate structures, leading to a stronger physical component of the plasma etching. This might increase the plasma-damage of the silicon sub-surface layer and hence lower the carrier lifetimes. We believe that optimizing the plasma-induced damage layer is equally as important as having a good surface passivation layer.

In conclusion, we fabricated optimized b-Si structures that absorb more than 91% of the theoretically possible fraction of photons of the Yablonovitch limit in the wavelength range between 300 nm and 1150 nm. Under optimum conditions, these structures exhibit similar effective carrier lifetimes like polished wafers. By varying the etching conditions to produce different b-Si structures, we found that a low plasma damage to the sub surface layer is as important for long carrier lifetimes as a good electronic passivation of the surface. By using an annealed 100 nm thick conformal Al_2O_3 layer on the surface and by optimizing the plasma etching conditions to obtain maximum optical scattering with low plasma-induced damage, the surface recombination velocities have been reduced down to $S_{eff} \leq 13 \pm 2$ cm/s. Our findings might enable high efficiency passivated emitter and rear contact (PERC) solar cells.

The authors acknowledge funding from the German Federal Ministry of Education and Research within the project PHIOBE and the Research College STRUKTSOLAR.

[1]E. Yablonovitch, J. Opt. Soc. Am. **72**, 899 (1982).
[2]M. Kroll, T. Käsebier, M. Otto, R. Salzer, and R. Wehrspohn, Proc. SPIE, **7725** (2010).
[3]M. Kroll, M. Otto, T. Käsebier, K. Füchsel, R. B. Wehrspohn, E.-B. Kley, A. Tünnermann, and T. Pertsch, Proc. SPIE, **8438** (2012).
[4]S. Schaefer and R. Lüdemann, J. Vac. Sci. Technol., A **17**, 749 (1999).
[5]S. H. Zaidi, D. S. Ruby, and J. M. Gee, IEEE Trans. Electron. Dev. **48**, 1200 (2001).
[6]K. Füchsel, A. Bingel, N. Kaiser, and A. Tünnermann, Proc. SPIE **8065** (2011).
[7]K. Füchsel, M. Kroll, T. Käsebier, M. Otto, T. Pertsch, E.-B. Kley, R. B. Wehrspohn, N. Kaiser, and A. Tünnermann, Proc. SPIE **8438** (2012).
[8]J. Yoo, G. Yu, and J. Yi, Mater. Sci. Eng., B **159–160**, 333 (2009).
[9]J. Zhao, A. Wang, P. P. Altermatt, S. R. Wenham, and M. A. Green, Sol. Energy Mater. Sol. Cells **41–42**, 87 (1996).
[10]R. Hezel and K. Jaeger, J. Electrochem. Soc. **136**, 518 (1989).
[11]B. Hoex, S. B. S. Heil, E. Langereis, M. C. M. van de Sanden, and W. M. M. Kessels, Appl. Phys. Lett. **89**, 042112 (2006).
[12]B. Hoex, J. J. H. Gielis, M. C. M. van de Sanden, and W. M. M. Kessels, J. Appl. Phys. **104**, 113703 (2008).
[13]B. Hoex, M. C. M. van de Sanden, J. Schmidt, R. Brendel, and W. M. M. Kessels, Phys. Status Solidi RRL **6**, 4 (2012).
[14]M. Knez, K. Nielsch, and L. Niinistö, Adv. Mater. **19**, 3425 (2007).
[15]F. Werner, B. Veith, D. Zielke, L. Kühnemund, C. Tegenkamp, M. Seibt, R. Brendel, and J. Schmidt, J. Appl. Phys. **109**, 113701 (2011).
[16]V. Naumann, M. Otto, C. Hagendorf, and R. B. Wehrspohn, J. Vac. Sci. Technol., A **30**, 04D106 (2012).
[17]G. Dingemans, W. Beyer, M. C. M. van de Sanden, and W. M. M. Kessels, Appl. Phys. Lett. **97**, 152106 (2010).

[18]H. Jansen, M. de Boer, R. Legtenberg, and M. Elwenspoek, J. Micromech. Microeng. **5**, 115 (1995).
[19]M. Otto, M. Kroll, T. Käsebier, S.-M. Lee, M. Putkonen, R. Salzer, P. T. Miclea, and R. B. Wehrspohn, Adv. Mater. **22**, 5035 (2010).
[20]G. Dingemans, R. Seguin, P. Engelhart, M. C. M. van de Sanden, and W. M. M. Kessels, Phys. Status Solidi RRL **4**, 10 (2009).
[21]D. A. Clugston and P. A. Basore, Prog. Photovoltaics **5**, 229 (1997).
[22]M. A. Green, Sol. Energy Mater. Sol. Cells **92**, 1305 (2008).